Article

Not peer-reviewed version

Study on the Near-Distance Object Following Performance of a 4WD Crop Transport Robot: Application of 2D LiDAR and Particle Filter

Eun-Seong Pak , Byeong-Hun Kim , Kil-Soo Lee , Yong-Chul Cha , Hwa-Young Kim *

Posted Date: 28 November 2024

doi: 10.20944/preprints202411.2241.v1

Keywords: LiDAR Sensor; Target Tracking; Particle Filtering; Proportional-Derivative Controller; Agricultural Produce Transportation

Article

Study on the Near-Distance Object Following Performance of a 4WD Crop Transport Robot: Application of 2D LiDAR and Particle Filter

Eun-Seong Pak [1], Byeong-Hun Kim [2], Kil-Soo Lee [1], Yong-Chul Cha [1] and Hwa-Young Kim [3,*]

[1] Korea Construction Equipment Technology Institute, 36, Sandan-ro, Gunsan-si, Jeonbuk-do, Republic of Korea
[2] DeepLink, 96, Banyeo-ro, Haeundae-gu, Busan, 48036, Republic of Korea
[3] School of Mechanical Engineering, Pusan National University, 2, Busandaehak-ro 63beon-gil, Geumjeong-gu
* Correspondence: hyokim@pusan.ac.kr; Tel.: +82-052-510-2861

Abstract: In this paper, the development and performance evaluation of a 4WD robot system designed to follow near-distance moving objects using a 2D LiDAR sensor are presented. The study incorporates identifier (ID) classification and a distance-based dynamic angle of perception model to enhance the tracking capabilities of the 2D LiDAR sensor. A particle filter algorithm was utilized to verify the accuracy of object tracking. Furthermore, a Proportional-Derivative (PD) controller was designed and implemented to ensure the stability of the robot during operation. Experimental results demonstrate the potential applicability of these approaches in various industrial applications.

Keywords: LiDAR Sensor; Target Tracking; Particle Filtering; Proportional-Derivative Controller; Agricultural Produce Transportation

1. Introduction

The global agricultural landscape has undergone significant changes in recent years, driven by rising environmental concerns and the evolving needs of a more health-conscious population. As consumer awareness about sustainable farming and the health benefits of organically grown produce has increased, there has been a parallel rise in interest toward improving agricultural systems that support environmentally friendly practices [1,8]. Climate change has also introduced significant challenges, altering growing conditions and putting strain on existing farming practices, which necessitates resilient farming solutions [3]. In South Korea, the agricultural sector faces additional challenges due to the decreasing and aging workforce, leading to a significant labor shortage [9]. This shortage directly impacts agricultural productivity and sustainability, emphasizing the urgent need for automation and mechanization in farming practices. Furthermore, the country's compact and rugged terrains, characterized by narrow and confined furrows between crop rows, limit the effectiveness of traditional large-scale agricultural machinery. As a result, there is a growing market need for innovative solutions that can enhance productivity while adapting to these unique geographical constraints. These dynamics have emphasized the importance of smart, adaptable technologies that support sustainable practices while minimizing environmental footprints [8]. Recognizing this market demand, our research project aims to develop small mobile robots specifically designed for transporting crops in challenging outdoor environments. Small mobile robots have emerged as a promising solution to address both labor shortages and the limitations posed by the terrain. They offer specific advantages over traditional machinery, such as reducing soil compaction, enhancing energy efficiency, and operating flexibly in confined spaces. This is particularly crucial in Republic of Korea, where mobility in narrow spaces is essential for efficient farming operations. Technological advances in autonomous navigation and machine learning have

Preprints.org (www.preprints.org) | NOT PEER-REVIEWED | Posted: 28 November 2024 doi:10.20944/preprints202411.2241.v1

enabled the development of agricultural robots with enhanced efficiency and precision. These robots are now capable of operating effectively in complex outdoor environments. Innovations in LiDAR-based perception, vision systems, and multi-modal data integration are key to enhancing robots' ability to navigate farm paths effectively [2,6]. Research has shown that these technologies can significantly reduce labor-intensive tasks and increase productivity in precision farming [3,6]. Consequently, with a growing emphasis on reducing labor needs particularly in countries like South Korea robotics has emerged as a promising solution [7].

Figure 1 illustrates examples of crop transportation equipment in the Republic of Korea, highlighting the need for improved mobility and automation. This study utilizes a low-spec 2D LiDAR sensor to develop a system capable of effectively following objects in close proximity within an outdoor agricultural setting, aiming to enhance the practicality of small mobile robots in such environments. With the recent advancements in machine learning and robotic systems, recognition and classification technologies of human forms utilizing various sensor data have become important research areas. In this context, two-dimensional (2D) LiDAR (Light Detection and Ranging) has emerged as a widely used technology in various applications such as personal and industrial robots and autonomous vehicles due to its advantages of being relatively inexpensive and capable of sensing a wide range. This technology excels at quickly scanning and mapping the surrounding environment and is essential for recognizing dynamic objects like humans in safety-related industries [11–17]. Figure 2 illustrates various applications of LiDAR sensors, demonstrating their versatility and importance in modern robotic systems.

Figure 1. Examples of agricultural product transportation methods in Republic of Korea.

Preprints.org (www.preprints.org) | NOT PEER-REVIEWED | Posted: 28 November 2024 doi:10.20944/preprints202411.2241.v1

Figure 2. Applications of LiDAR Sensors: Positioning Aid for Container Handling, Navigation Aid and Collision Prevention for Cranes, Vehicle Classification, and Monitoring Open Spaces for Building Security.

LiDAR sensing technology can be broadly categorized into two-dimensional (2D) and three-dimensional (3D) systems, enabling rapid information acquisition through distance and angular resolution. While single-channel 2D LiDAR scanners offer a cost-effective solution, their lower specifications can limit perception performance without the implementation of sophisticated algorithms and data processing methods. On the other hand, high-performance LiDAR sensors are often used for perception in autonomous vehicles, providing superior specifications but coming at a relatively high cost [18]. Table 1 compares the specifications of the YDLiDAR-G6 sensor used in this study with those of other leading LiDAR sensors. As shown, LiDAR sensors from SICK and Velodyne provide a detection range of over 80 meters with high resolutions of 0.167° and 0.11°, respectively, but their size and cost pose challenges for small mobile robot applications. In contrast, the YDLiDAR-G6 sensor offers a cost-effective solution with sufficient key functionalities suitable for such applications

Table 1. Comparison of LiDAR Sensor Specifications.

Items	YD LiDAR-G6	SICK-LMS	Velodyne Alpha Prime
Number of Channels	Single	Single	128 channels
Field of View (Horizontal)	360°	190°	360°[1]
Maximum Distance	16 meters	80 meters	245 meters
Angular Resolution	0.1°, 0.14°, 0.24°	0.042°,0.083°, 0.1667°,0.25°, 0.333°,0.5°, 0.667°, 1°	Minimum 0.11°
Protocol	Serial	TCP/IP, UDP/IP	TCP/IP, UDP/IP
Price	About 300 dollars	About 10,000 dollars	About 70,000 dollars

This research was conducted to develop a near-distance object-following system using a relatively low-spec. 2D LiDAR sensor for a crop transport platform suitable for the unique outdoor agricultural conditions in South Korea, and to analyze its performance. Through this study, we have observed the potential feasibility of the system in practical applications. We plan to conduct tests in

Preprints.org (www.preprints.org) | NOT PEER-REVIEWED | Posted: 28 November 2024 doi:10.20944/preprints202411.2241.v1

actual field environments within South Korea to further explore its usability and effectiveness for real- environment agricultural applications.

2. System Configuration

Figure 3 illustrates the robot, sensors, and controllers used in this study. The Scout2.0 robot from Agile X, which can be controlled via an open-source ROS (Robotics Operating System) platform, was chosen for its versatility across various industrial applications [19]. The robot is driven by four fixed wheels, employing a skid-steer mechanism. The distance between the wheels is 0.49 m, and the width is 0.69 m, allowing longitudinal and lateral control through the adjustment of wheel RPMs. The total weight is approximately 60 kg, and the robot can carry up to 50 kg of payload. The object-following sensor used was the G6 model from YD-LiDAR, which has a 360° field of view and an angular resolution of 0.1°, with each particle being measured at 10 kHz. The minimum detection range is 0.12 m, and the maximum range is 16 m The sensor was mounted at a height of 0.4 m from the ground, facing forward. The controller used in this study was the NVIDIA Jetson AGX Orin board, running on Ubuntu 20.04 LTS and ROS [20]. A Python-based program was developed for sensor data acquisition and analysis, enabling object-following and PD control in both longitudinal and lateral directions.

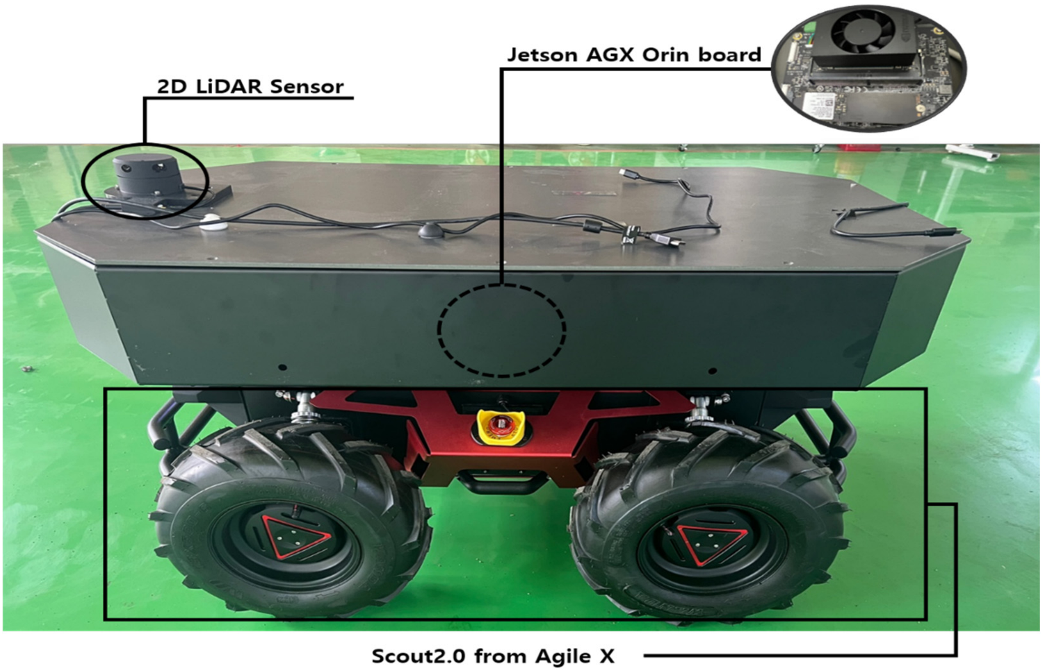

Figure 3. The controller, sensors, and robot platform used in the experiment.

3. Mobile Object-Following System Using LiDAR

3.1. Object Classification Using Density-Based Clustering

The density-based clustering technique identifies objects by clustering data points from the LiDAR sensor based on spatial density, determining the continuity of points around a data point using density within a defined radius. This approach is particularly effective when using data from low-specification LiDAR sensors [21]. As shown in Figure 3, a given data point ‘p’ is considered a neighbor if at least one additional ‘p’ exists within a radius ‘ε’.

By setting ‘ε’ to a value within 0.05 m for the target object in front of the LiDAR sensor, continuous objects could be identified, as confirmed by the distribution of points shown in Figure 4.

Preprints.org (www.preprints.org) | NOT PEER-REVIEWED | Posted: 28 November 2024 doi:10.20944/preprints202411.2241.v1

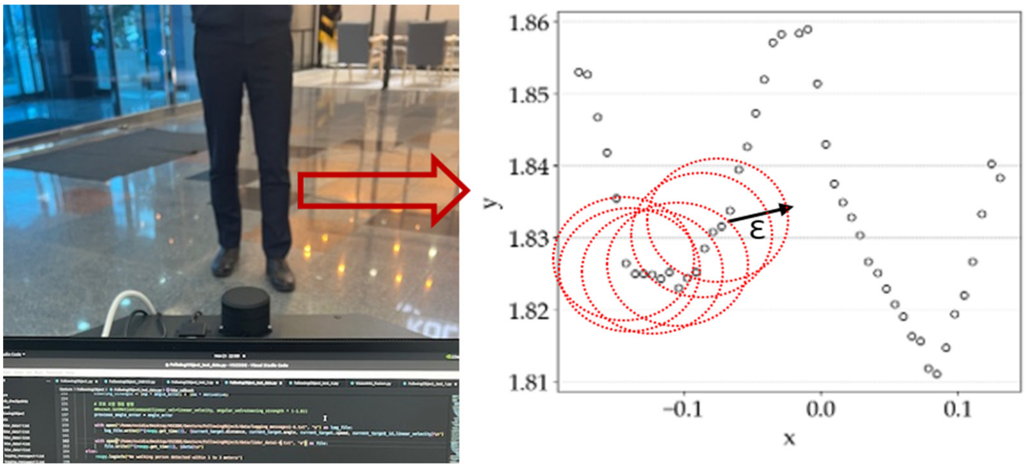

Figure 4. LiDAR sensor data point distribution and density-based clustering method.

3.2. Object Detection and Visualization

The message system in ROS (Robot Operating System) is a core mechanism for data communication between nodes. ROS messages are simple data structures that follow a defined format with a series of fields. The 2D LiDAR sensor collects and processes data through a ROS node, continuously publishing distance data about the surrounding environment to ROS. This data is represented in the 'sensor_msgs/LaserScan' message format. This message type includes the following information about the LiDAR scan.

Table 2. ROS message type includes the following information about the LiDAR scan.

Type	Messages
header	Includes the message's timestamp and frame ID
angle_min	The angle at which the scan starts
angle_max	The angle at which the scan ends.
range_min	The minimum distance the LiDAR can detect
range_max	The maximum distance the LiDAR can detect
ranges	An array of distance data, Each element represents the distance measured from the LiDAR

The controller receives distance and angle data from reflected LiDAR points and analyzes sequential data points to identify follow able objects. This process involves detecting the width of continuous objects that meet threshold conditions and generating object data based on compliant points. Real-time visualization of object information was achieved using the ROS open-source software RViz, as shown in Figure 5, enabling intuitive understanding of the distance and orientation of objects relative to the robot, as well as distinguishing additional objects. Figure 6, provided real-time insight into sensor readings, offering detailed monitoring and analysis capabilities for data gathered from the LiDAR sensors.

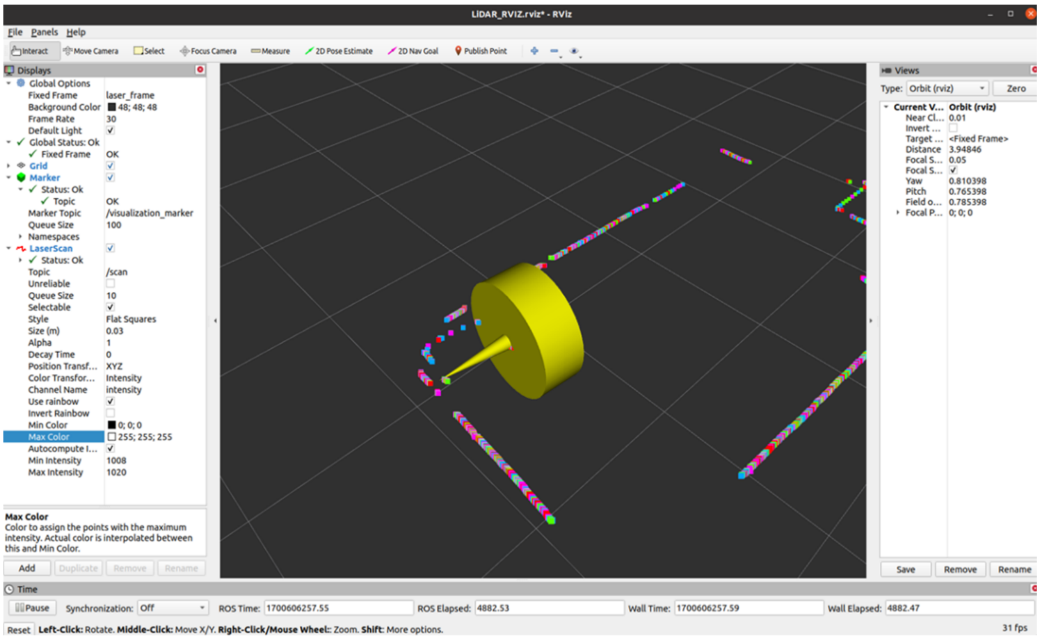

Figure 5. 3D Visualization of a tracked object using ROS RViz.

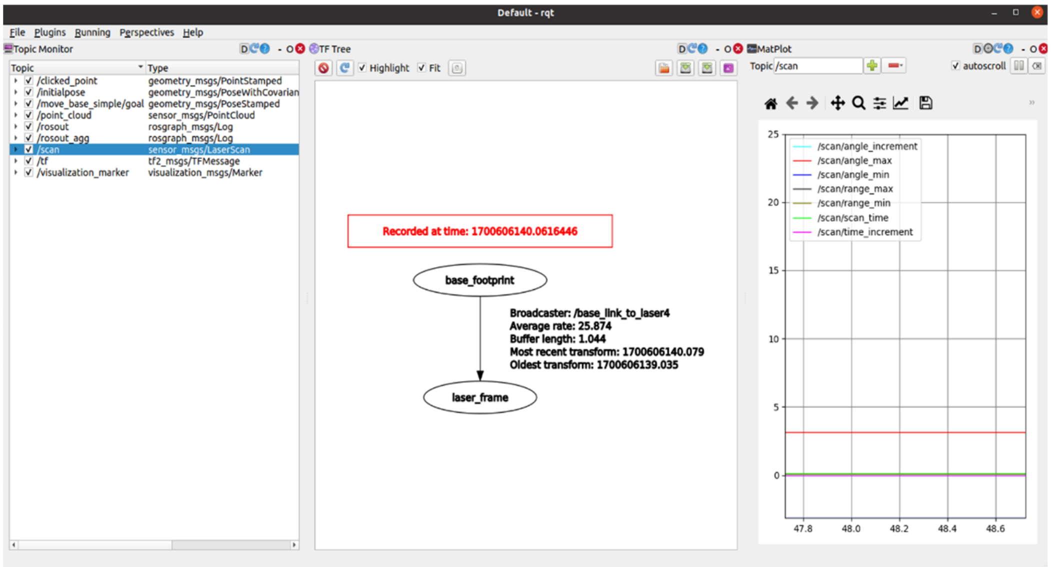

Figure 6. Monitoring LiDAR sensor data using ROS RQT.

3.3. Object Identifier (ID) Classification

Due to the characteristics of outdoor fields in the Republic of Korea, where multiple objects besides the target object may be present, initial detected objects were assigned identifiers to maintain tracking continuity [22]. Dynamic objects detected subsequently were also assigned identifiers to differentiate them from the initial object. Figures 7 and 8 illustrate the logic for real-time updating of identifiers and maintaining object tracking during robot navigation, along with the corresponding pseudocode. This approach ensured that the robot consistently followed the initial object, regardless of newly detected objects.

Preprints.org (www.preprints.org) | NOT PEER-REVIEWED | Posted: 28 November 2024 doi:10.20944/preprints202411.2241.v1

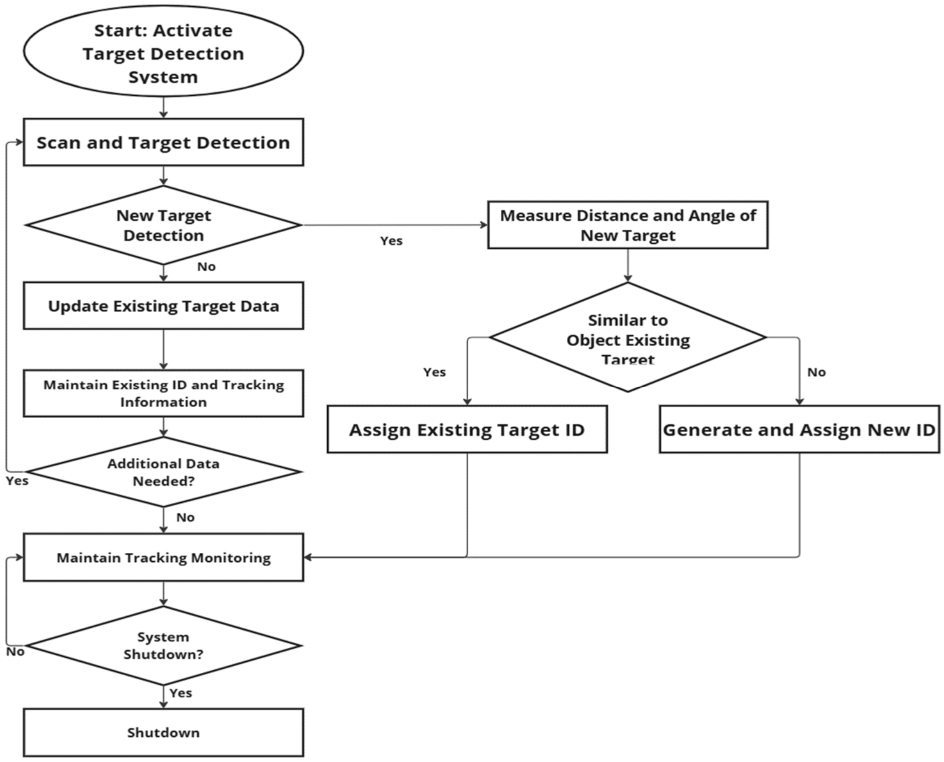

Figure 7. Flowchart for classification of tracking object identifiers.

Algorithm 1 Target Detection System Pseudocode

```
START
// Activate Target Detection System
ACTIVATE_Target_Detection_System()
while TRUE do
    SCAN_And_Target_Detection()
    if New_Target_Detected then
        Measure_Distance_And_Angle_Of_New_Target()
        if Similar_To_Existing_Target then
            Assign_Existing_Target_ID()
        else
            Generate_And_Assign_New_ID()
        end if
    else
        Update_Existing_Target_Data()
        Maintain_Existing_ID_And_Tracking_Information()
    end if
    if Additional_Data_Needed() then
        // Continue monitoring and updating
        CONTINUE
    else
        Maintain_Tracking_Monitoring()
    end if
    if System_Shutdown() then
        SHUTDOWN()
        BREAK
    end if
end while
END
```

Figure 8. Tracked object identifier classification pseudocode.

Preprints.org (www.preprints.org) | NOT PEER-REVIEWED | Posted: 28 November 2024 doi:10.20944/preprints202411.2241.v1

3.4. Angle Adjustment Based on Distance for Optimal Tracking

A mechanism for dynamically adjusting the perception angle range based on the relative distance to the target was implemented for the object-following process using the LiDAR sensor. Given the frequent presence of obstructive elements in outdoor fieldwork and the increased potential for object loss as distance increases, it is essential for the platform to maintain high close-range tracking performance [23–25]. Therefore, a broader angle range was applied as the target moved closer to ensure it remained within the detection range.

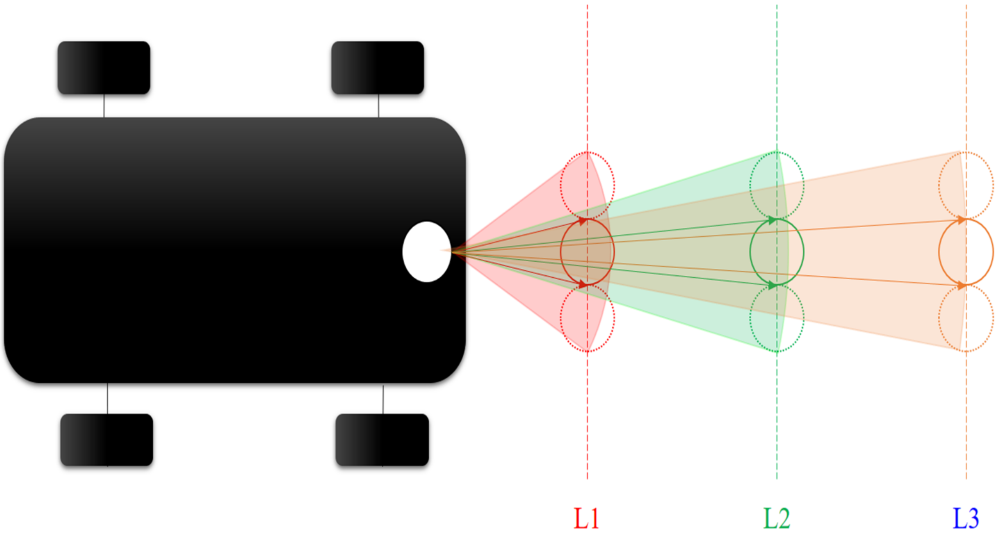

Figure 9. Angle adjustment based on distance for optimal tracking diagram.

For instance, as shown in Figure 8, the range from 0.7 m to 1.0 m from the robot was defined as 'L1', where a wide angle of ±45° was applied. For distances of 1.0 m to 1.5 m ('L2'), an angle range of ±30° was set, and for distances exceeding 1.5 m ('L3'), a narrower range of ±15° was applied.

4. Particle Filter Model for Experiments

The particle filter is a widely used algorithm for object tracking, suitable for non-linear and non-Gaussian systems [26].

4.1. Initialization Process

To process LiDAR data and calculate the relative direction between the target and the robot, a particle filter algorithm was employed. The initialization process involved creating 50 particles with random initial states. The particles' distances followed a uniform distribution between 0.5 m and 1.0 m, and the angles ranged from −π to π.

$$R_0^{(i)}\ Uniform(0.5, 1.0), \theta_0^{(i)}\ Uniform(-\pi, \pi) \quad (1)$$

In Equation 1, $R_0^{(i)}$ represents the distance to the object, and $\theta_0^{(i)}$ represents the angle Distance R_0 as uniformly distributed between 0.5m and 1.0m, and angle θ_0 was distributed between −π and π, under the assumption that the target is located around the robot. Through an estimation process based on actual measurement data, the estimated position gradually converged to higher accuracy.

4.2. Weight Calculation and Update

At each measurement step, the distance and angle measurements from the LiDAR were used to calculate errors and update particle weights using a normal distribution probability density function [27]. The noise standard deviation for distance measurements was set to 0.1, and for angle measurements to pi/36.

Preprints.org (www.preprints.org) | NOT PEER-REVIEWED | Posted: 28 November 2024 doi:10.20944/preprints202411.2241.v1

$$\omega_t^{(i)} = \frac{1}{\sqrt{2\pi\sigma^2}} e^{-\frac{(z_t - h(x_t^{(i)}))^2}{2\sigma^2}} \tag{2}$$

particle's weight using the probability density function of the normal distribution. Here, z_t is the actual measurement value from LiDAR, $h\left(x_t^{(i)}\right)$ is the expected measurement value based on the particle state, and σ is the standard deviation of measurement noise. This means that the difference between actual and expected measurements is normalized by the standard deviation of noise, determining the weight based on how closely the particle matches the measurement data.

4.3. Resampling and State Estimation

After weight updates, resampling was performed to remove particles with low weights and replicate those with higher weights.

$$x_{t+1} = \frac{\sum_{i=1}^{N} \omega_t^{(i)} x_t^{(i)}}{\sum_{i=1}^{N} \omega_t^{(i)}} \quad a = 1, \tag{3}$$

Equation 3 represents the resampling process, where the new state estimate is calculated as the weighted average of the particles, minimizing uncertainty and focusing on accurate target tracking.

5. Design of Longitudinal and Lateral PD Controllers

Using the calculated direction and distance between the target and the robot as direct control inputs can lead to excessive overshoot, negatively impacting driving performance [28]. To address this, a proportional-derivative (PD) controller is designed to reduce overshoot and ensure robust transient response, as shown in Figure 10 [29]. The PD controller generated direction and speed control inputs in real-time based on the distance and angle of the target. The transfer functions for each process are represented by Equations 4 and 5.

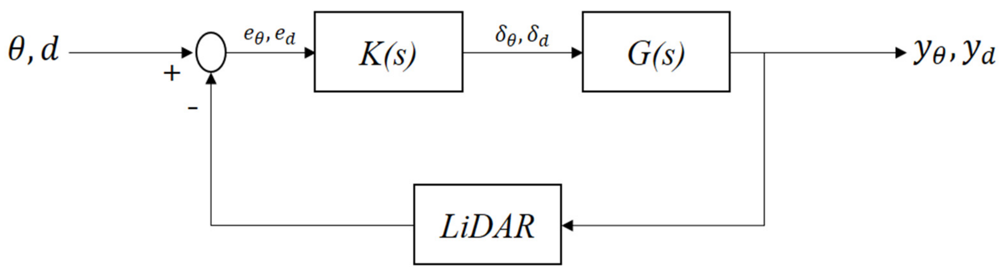

Figure 10. Flowchart of longitudinal and lateral PD controllers.

$$K(s) = K_p + K_d \tag{4}$$

$$T(s) = \frac{G(s)(K_p + K_d)}{1 + G(s)(K_p + K_d)} \tag{5}$$

Figure 11 shows that simulation results with $\boldsymbol{K_p}$ set to 0.5 and $\boldsymbol{K_d}$ set to 0.3 showed that the PD controller effectively reduced oscillations and allowed for rapid convergence to zero, outperforming basic proportional control.

 doi:10.20944/preprints202411.2241.v1

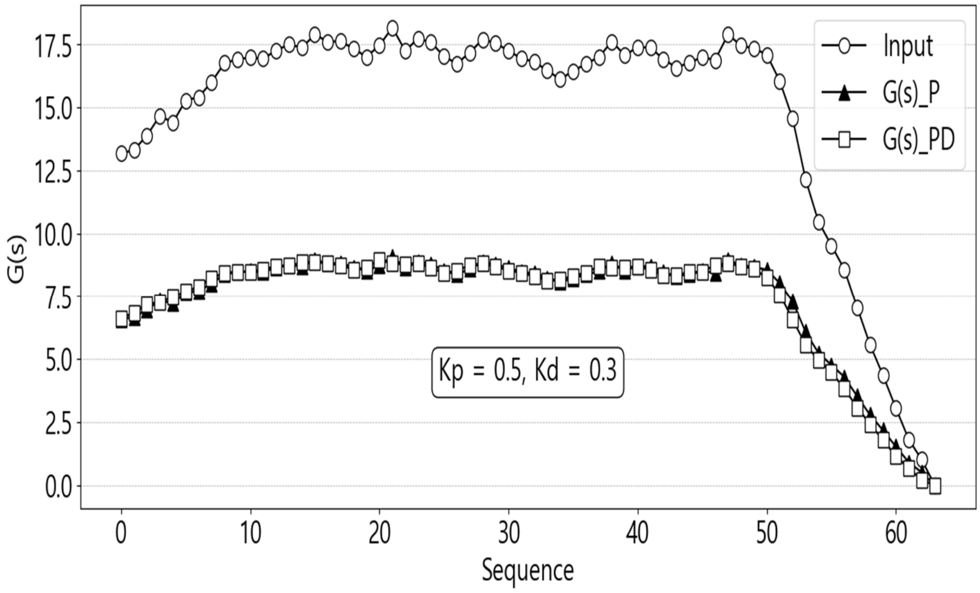

Figure 11. This is a figure. Schemes follow the same formatting.

6. Experimental Methods

The experimental setup is shown in Figures 12 and 13. Experiment 1 involved navigating a 1.5 m wide corridor in a straight path, passing through two narrow 1 m paths, and returning to the starting point to assess the effect of obstacle interference on tracking performance. Experiment 2 tested the ability to maintain tracking through two 0.4 m wide obstacles placed diagonally with a 1 m gap between them. This evaluated the system's capability to retain the initial target while searching for additional objects during straight-line tracking. The moving object was a human walking at an average speed of 4 km/h.

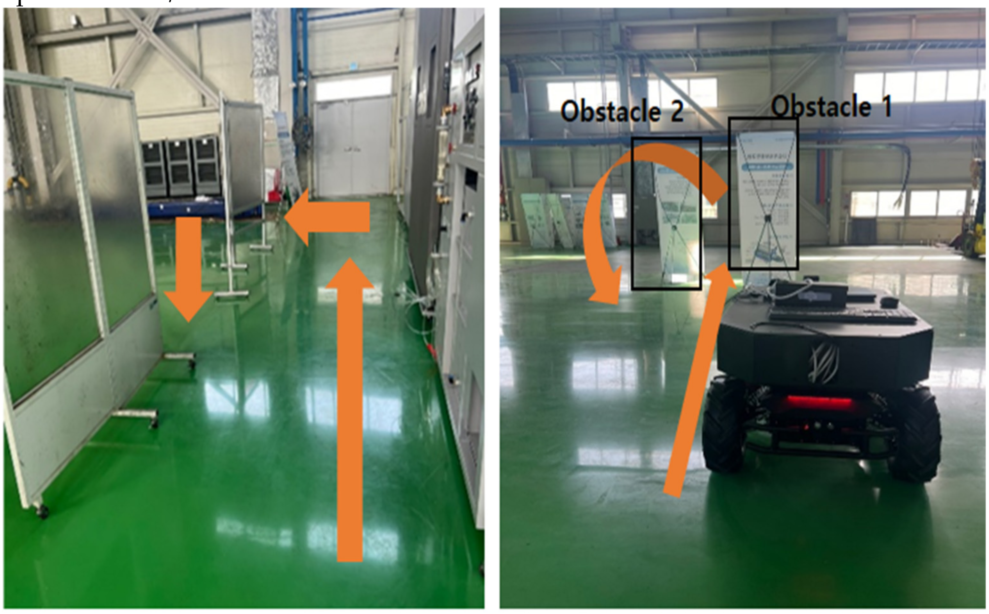

Figure 12. Experimental environment for two paths.

Preprints.org (www.preprints.org) | NOT PEER-REVIEWED | Posted: 28 November 2024 doi:10.20944/preprints202411.2241.v1

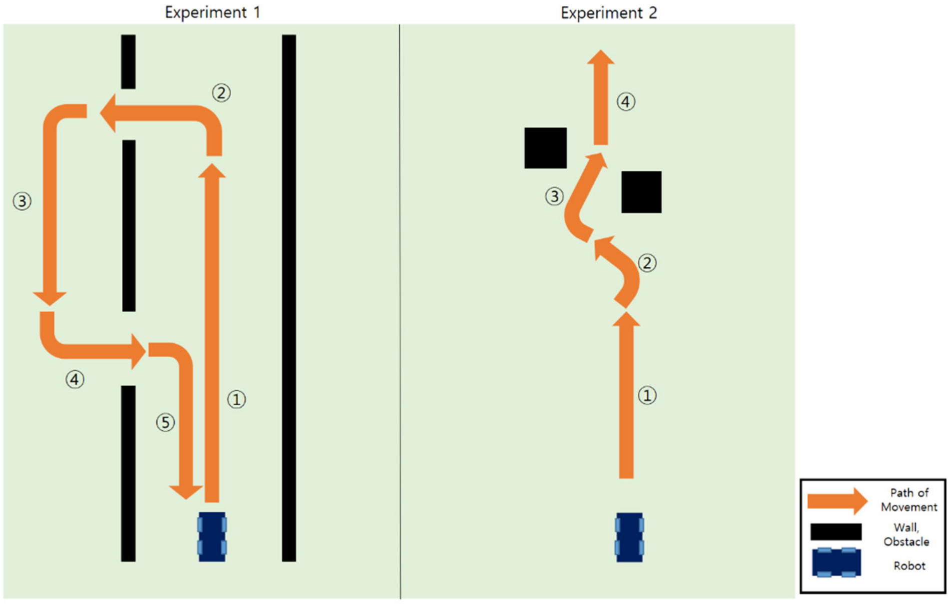

Figure 13. Follow driving experiment scenario.

7. Experimental Results

The angle between the robot and the tracked object, calculated in real-time from the LiDAR sensor, was defined as the actual angle, while the angle estimated through the particle filter was defined as the estimated angle. The baseline angle (0 rad) indicated a direct alignment between the robot and the object.

Figure 14 shows the change in angle between the robot and the target during Experiment 1. To facilitate analysis, data were divided into five courses with key points. A comparison of the median values with the reference angle showed that the estimated results performed 0.01 rad better in course 1 and 0.02 rad. better in course 2. Additionally, fewer outliers were observed in course 5.

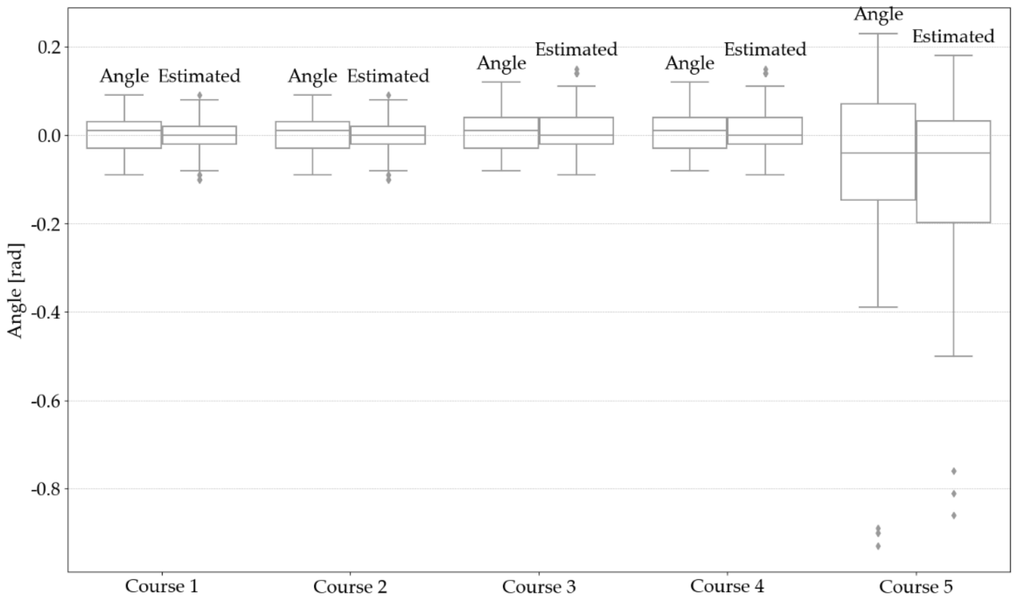

Figure 14. Comparison of actual and estimated (particle filter) angle values from experiment 1.

Figure 15 compares the actual and estimated distance values during Experiment 1. The median values of actual and estimated distances were found to be similar or identical in most courses, with few outliers.

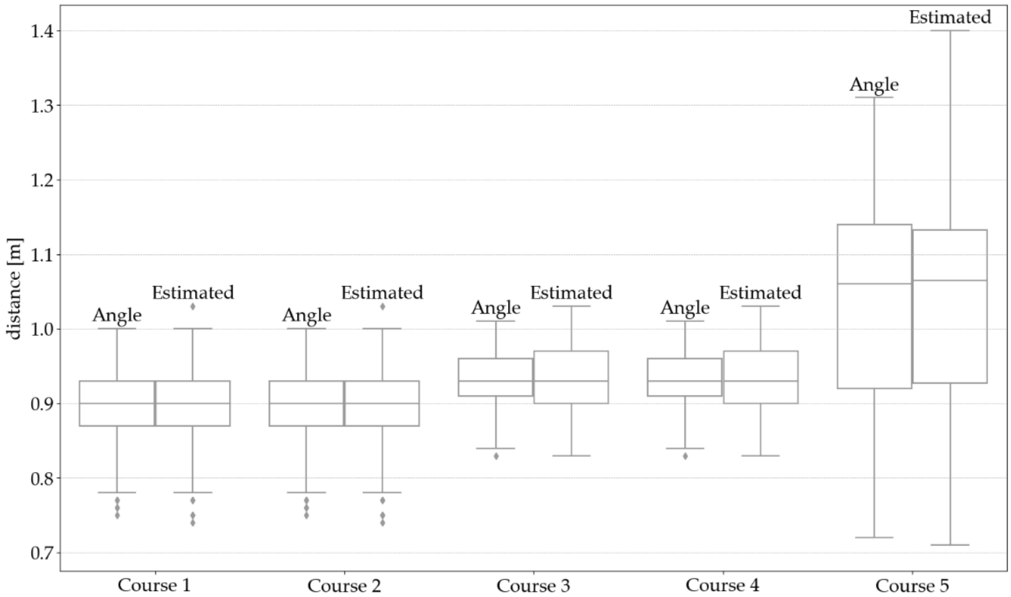

Figure 15. Comparison of actual and estimated (particle filter) distance values from experiment 1.

Figures 16 and 17 display results similar to those of Experiment 1, showing a 0.01 rad median improvement in course 1 and 4, with other courses progressing identically. Distance median values were either the same or showed minimal differences, which were not statistically significant.

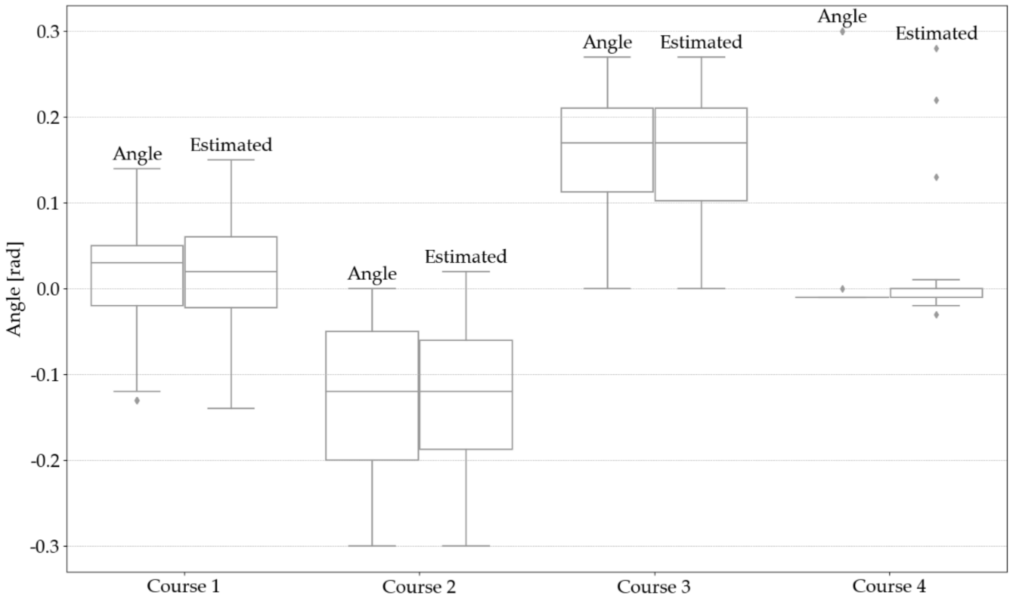

Figure 16. Comparison of actual and estimated (particle filter) angle values from experiment 2.

 doi:10.20944/preprints202411.2241.v1

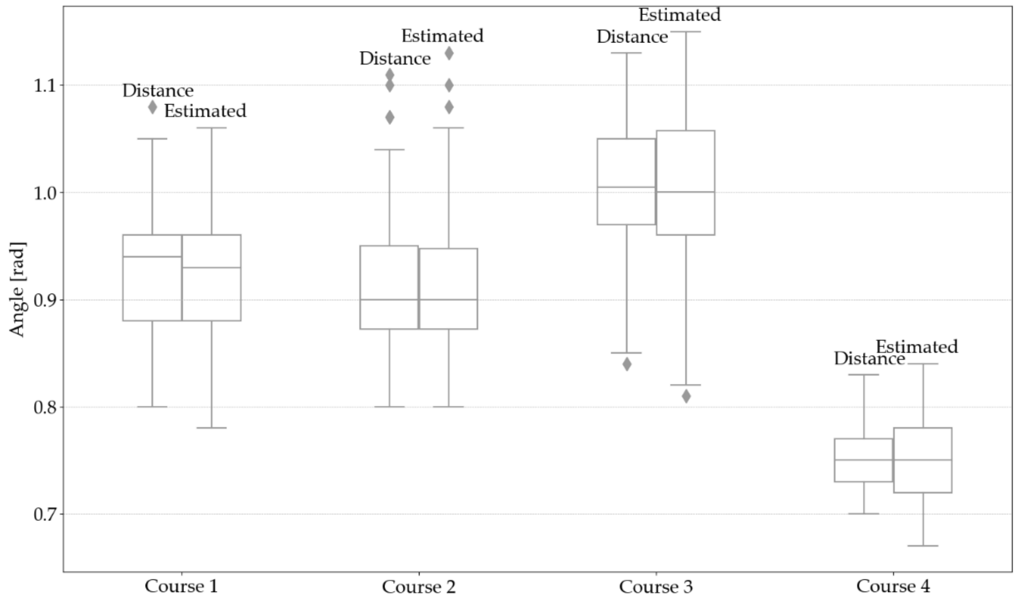

Figure 17. Comparison of actual and estimated (particle filter) angle values from experiment 2.

Based on Experiments 1 and 2, as shown in Figures 18 and 19, the final evaluation of the robot's longitudinal and lateral tracking performance confirmed that the robot maintained a reasonable distance while moving without deviating excessively from the path. The average tracking distance in Experiment 1 was 1.02m, and the average tracking angle was 0.563 rad., with standard deviations of 0.022m and 0.083 rad, indicating minimal variability due to human movement. Experiment 2 yielded an average of 0.967m and 0.287 rad., with standard deviations of 0.005m and 0.069 rad., showing similar results to Experiment 1.

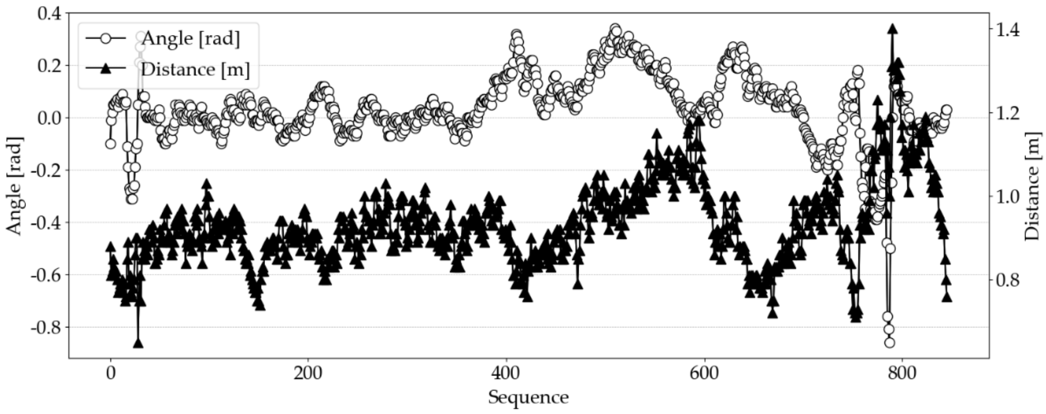

Figure 18. Tracking performance results of experiments 1.

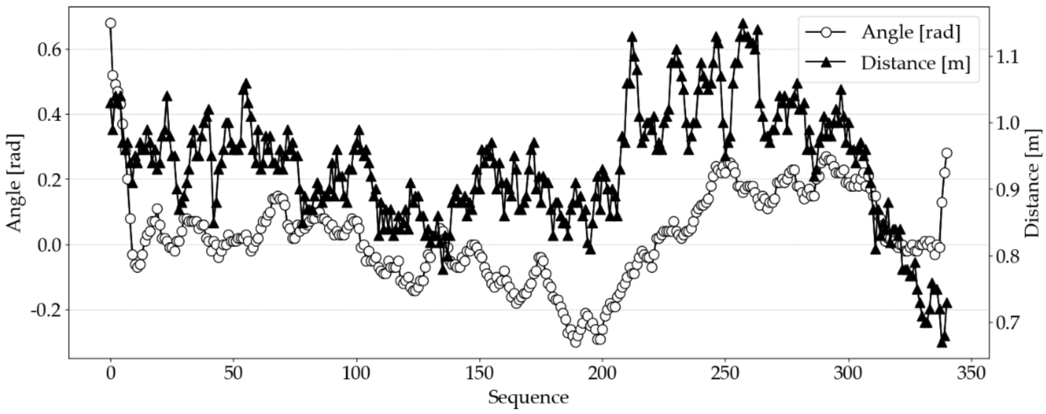

Figure 19. Tracking performance results of experiments 2.

8. Conclusion and Discussion

This research developed and evaluated a 4WD robot platform for near-distance moving object tracking using a relatively low-spec. 2D LiDAR sensor. The integration of ID classification and a distance-based dynamic recognition angle model improved the object-tracking performance of the LiDAR sensor. The implementation of a particle filter algorithm further validated the system's tracking capabilities. Additionally, the PD controller ensured the driving stability of the robot, as confirmed through performance experiments. The experimental results demonstrated the potential for effective data processing of the LiDAR sensor in near-distance object tracking, alongside stable driving performance of the 4WD mobile robot. This research contributes to the advancement of small-scale autonomous systems for agricultural use by addressing both economic and labor challenges in compact and rugged terrains. To further assess the system's practicality, future work will involve conducting tests in actual field environments to validate its usability and effectiveness in real-world agricultural settings. Additionally, future research should focus on enhancing data processing for increased complexity, such as medium and long-range navigation with more obstacles, and exploring dynamic adjustment of perception angles to improve system adaptability to changing environments.

Funding: This research was supported by the "2024 Technology Commercialization Support Project" (RS-2024-00349535: Development of a 12V electric Air Drill precision seeder for multi-seed rotavator attachment based on cloud control and embedded) funded by the Ministry of Agriculture, Food and Rural Affairs of Korea.

References

1. **Shamshiri, R.R.; Weltzien, C.; Hameed, I.A.; Yule, I.J.; Grift, T.E.; Balasundram, S.K.; Pitonakova, L.; Ahmad, D.; Ehsani, R.** Research and Development in Agricultural Robotics: A Perspective of Digital Farming. *Int. J. Agric. Biol. Eng.* **2018**, *11*, 1–14.
2. **Lee, W.S.; Ehsani, R.** Sensing Technologies for Precision Specialty Crop Production. *Comput. Electron. Agric.* **2015**, *114*, 2–9.
3. **Blackmore, S.; Stout, B.; Wang, M.; Runov, B.** Robotic Agriculture—The Future of Agricultural Mechanisation? In *Proceedings of the 5th European Conference on Precision Agriculture*, Uppsala, Sweden, 9–12 June 2005.
4. **Bac, C.W.; van Henten, E.J.; Hemming, J.; Edan, Y.** Harvesting Robots for High-Value Crops: State-of-the-Art Review and Challenges Ahead. *J. Field Robot.* **2014**, *31*, 888–911.
5. **Oksanen, T.; Visala, A.** Coverage Path Planning Algorithms for Agricultural Field Machines. *J. Field Robot.* **2009**, *26*, 651–668.
6. **Cheein, F.A.A.; Carelli, R.** Agricultural Robotics: Unmanned Robotic Service Units in Agricultural Tasks. *IEEE Ind. Electron. Mag.* **2013**, *7*, 48–58.
7. **Bechar, A.; Vigneault, C.** Agricultural Robots for Field Operations: Concepts and Components. *Biosyst. Eng.* **2016**, *149*, 94–111.
8. **Jin, X.; Li, Z.; Ji, S.; Yang, G.** Recent Advances in Crop Growth Monitoring Using Unmanned Aerial Vehicles. *Remote Sens.* **2021**, *13*, 3104.
9. OECD. Agricultural Policy Monitoring and Evaluation 2021: Addressing the Challenges Facing Food Systems; OECD Publishing: Paris, France, 2021.
10. Thrun, S.; Burgard, W.; Fox, D. Probabilistic Robotics; MIT Press: Cambridge, MA, USA, 2005.
11. **Mohamed, I.S.; Taha, A.M.; Elkilani, W.S.; Haggag, M.H.** Detection, Localization, and Tracking of Pallets Using Machine Learning Techniques and 2D Range Data. *Neural Comput. Appl.* **2020**, *32*, 8811–8828.
12. **Cha, D.; Chung, W.** Human-Leg Detection in 3D Feature Space for a Person-Following Mobile Robot Using 2D LiDARs. *Int. J. Precis. Eng. Manuf.* **2020**, *21*, 1299–1307.
13. **Yan, Z.; Duckett, T.; Bellotto, N.** Multisensor Online Transfer Learning for 3D LiDAR-Based Human Detection with a Mobile Robot. In *Proceedings of the 2018 IEEE/RSJ International Conference on Intelligent Robots and Systems (IROS)*; Madrid, Spain, 1–5 October 2018; pp. 763–768.
14. **Chen, G.; Sun, C.; Zhang, C.; Wang, W.; Li, Y.; Wu, X.** Pseudo-Image and Sparse Points: Vehicle Detection with 2D LiDAR Revisited by Deep Learning-Based Methods. *IEEE Trans. Intell. Transp. Syst.* **2021**, *22*, 7594–7605.
15. Kwon, S.-K.; Kim, K.-M.; Park, M.-H.; Song, J.-B**.** A New Human Detection Method Using Human Characteristic Functions of Low-Resolution 2D LiDAR. *J. Inst. Embed. Eng. Korea* **2016**, *11*, 267–276.

 doi:10.20944/preprints202411.2241.v1

16. **Luo, F.; Zhuang, Y.; Xie, L.; Yu, H.** Temporal Convolutional Networks for Multiperson Activity Recognition Using a 2-D LiDAR. *IEEE Internet Things J.* **2020**, *7*, 7432–7442.
17. **Chen, L.; Xiao, Y.; Lu, Y.; Zhang, X.** A Deep Learning-Based Method for Overhead Contact System Component Recognition Using Mobile 2D LiDAR. *Sensors* **2020**, *20*, 2313.
18. Jeong, J.-S.; Jang, J.-H.; Lee, J.-K. Trends in LiDAR Sensor Technology for Autonomous Vehicles. Auto J. Korean Soc. *Automot. Eng.* **2023**, 45(4), 22–26.
19. Scout2.0 Robot from Agile X. Available online: https://roas.co.kr/scout-2-0/ (accessed on 01 October 2024).
20. ROS (Robotics Operating System). Available online: https://www.ros.org/ (accessed on 01 September 2024).
21. Ester, M.; Kriegel, H.-P.; Sander, J.; Xu, X. A Density-Based Algorithm for Discovering Clusters in Large Spatial Databases with Noise. In Proceedings of the 2nd International Conference on Knowledge Discovery and Data Mining; Portland, OR, USA, **1996**; AAAI Press, pp. 226–231.
22. Li, Z.; Zhou, H.; Wang, W.; Ma, Q. Real-Time Detection, Tracking and Classification of Multiple Moving Objects in UAV Videos. In *Proceedings of the 2017 IEEE 29th International Conference on Tools with Artificial Intelligence (ICTAI)*, Boston, MA, USA, 6–8 November **2017**; pp. 614–621.
23. Holpp, M.; Dürr, L. Automatic Guidance System for Tractors in Fruit Farming. Swiss Federal Research Station for Agricultural Economics and Engineering Report **2006**, No. 631.
24. Shalal, N.; Low, T.; McCarthy, C.; Hancock, N. Orchard Mapping and Mobile Robot Localisation Using On-Board Camera and Laser Scanner Data Fusion - Part B: Mapping and Localization. Comput. Electron. Agric. **2015**, 119(1), 267–278.
25. Weiss, U.; Biber, P. Plant Detection and Mapping for Agricultural Robots Using a 3D LIDAR Sensor. Robotics and Autonomous Systems **2011**, 59(5), 265–273.
26. Arulampalam, M.S.; Maskell, S.; Gordon, N.; Clapp, T. A Tutorial on Particle Filters for Online Nonlinear/Non-Gaussian Bayesian Tracking. *IEEE Trans. Signal Process.* **2002**, 50(2), February.
27. Spiegel, M.R.; Stephens, L.J. Schaum's Outline of Theory and Problems of Statistics; McGraw Hill: New York, NY, USA, 1999.
28. Gehrig, S.K. A Trajectory-Based Approach for the Lateral Control of Car Following Systems. *IEEE Int. Conf. Proc.* **1997**, 596–601.
29. Kim, D.-W.; Hwang, H.-J. Design of Optimal PD Control System with Robust Performance. *J. Inst. Control Robot. Syst.* **1999**, 5(6), 656–666.